A&A 506, 993–997 (2009)
DOI: 10.1051/0004-6361/200912511

Astronomy & Astrophysics

New study of the quasi-molecular Lyman-γ satellites due to H-H$^+$ collisions

N. F. Allard[1], I. Noselidze[2], and J. W. Kruk[3]

[1] Observatoire de Paris, GEPI, UMR 8111, CNRS, 61, Avenue de l'Observatoire, 75014 Paris, France
e-mail: nicole.allard@obspm.fr
[2] Department of Physics, Tbilisi State University, Chavchavadze Avenue 3, 0128 Tbilisi, Georgia
[3] Department of Physics and Astronomy, Johns Hopkins University, Baltimore, MD 21218, USA

Received 16 May 2009 / Accepted 6 July 2009

ABSTRACT

Context. Quasi-molecular line satellites in the red wings of Lyman series of atomic hydrogen have been identified in the spectra of hydrogen-rich white dwarfs. These features are produced by radiative collisions.

Aims. Structures observed about 995 Å in the Lyman-γ wing of hot white dwarfs have been shown to be caused by quasi-molecular absorption of H_2^+ molecules.

Methods. Improvements to previous theoretical calculations of the Lyman-γ line profiles can be achieved by using a unified theory that takes into account the dependence of the dipole moments on internuclear distance during the collision.

Results. For the first time, we have computed the transition dipole moments. We measure a significant increase in the region of the formation of the satellites, which alters the general shape of the profile.

Conclusions. A large increase in the strength of the two main satellites at 992 and 996 Å leads to a deeper broad absorption in the synthetic spectra, which should improve the comparison with observation as previous predicted Lyman-γ satellites were too weak.

Key words. line: profiles – stars: white dwarfs

1. Introduction

Absorption features at 1400 Å and 1600 Å in the red wing of the Lyman-α line were first observed in the spectra of hydrogen-rich white dwarfs obtained with the *IUE* (International Ultraviolet Explorer) satellite (Greenstein 1980; Holm et al. 1985). They were explained as being caused by quasi-molecular absorption of the H_2 (1600 Å) or H_2^+ (1400 Å) molecules by Koester et al. (1985) and Nelan & Wegner (1985). Nevertheless quantitative agreement was not achieved until the work of Allard & Koester (1992) which adopted realistic molecular potentials. A theoretical approach using unified line broadening theory, the full complement of contributing states, and simultaneous perturbation by neutral atoms and ions was developed in Allard et al. (1994).

The application of the new profiles to *IUE* and *HST* (Hubble Space Telescope) provided much improved fits for the UV spectra of cool DA white dwarfs (e.g. Koester & Allard 1993; Bergeron et al. 1995). They also fit the spectra of laser-produced hydrogen plasmas (Kielkopf & Allard 1995).

One significant effect of these line satellites is the variation in the transition probability with the separation of the colliding atoms. The resulting profiles show that a large enhancement in the amplitude of a satellite occurs whenever the dipole moment increases across the region of internuclear distance where the satellite is formed. For particular examples, we refer the reader to Allard et al. (1998a) for a study of Lyman-α satellites and Allard et al. (1998b) for a study of Lyman-β satellites. This leads to a quantitative improvement of the synthetic spectra of λ Bootis stars compared to *IUE* observations (Allard et al. 1998c).

Subsequently, satellites in the red wing of Lyman-β were observed in the spectra of the DA white dwarf Wolf 1346 with the Hopkins Ultraviolet Telescope (*HUT*) (Koester et al. 1996). The H_2^+ satellite absorption features at 1058 Å and 1076 Å were observed in 4 other targets with Orbital Retrievable Far and Extreme Ultraviolet Spectograph (*ORFEUS*) (Koester et al. 1998). Lyman-β profiles of Allard et al. (1998b) were used by Koester et al. (1998) to successfully interpret these spectra.

Another strong feature close to 995 Å was also present in the *HUT* spectra of the DA white dwarf Wolf 1346 and distinctly detected in *FUSE* (Far Ultraviolet Spectograph Explorer) spectra of CD −38°10980 (Wolff et al. 2001) and Sirius B (Holberg et al. 2003). Theoretical calculations of the absorption profiles of Lyman-γ line based on accurate ab initio potentials were made by Allard et al. (2004b) to explain the observation of this feature.

The good agreement between the *FUSE* spectra and our calculations allowed the line satellites near 995 Å to be identified. The 995 Å feature is a blend of two quasi-molecular Lyman-γ satellites produced by H-H$^+$ collisions near 992 Å and 996 Å. The shape of the profile in the region of these line satellites is sensitive to their relative strength. It is therefore important to obtain an accurate quantitative determination of the satellite amplitudes. Accurate theoretical molecular potentials must be used to describe the interaction between the radiator and the perturber, as we did in the work described in Allard et al. (2004b). Another important factor, not included, was the variation in the dipole moment during the collision.

One of us (I. N.) has now computed dipole moments for H_2^+ as a function of internuclear distance for the transitions

involved in the Lyman-γ line. We describe these new calculations in Sect. 2.

In Sect. 3, we apply the unified theory (Allard et al. 1999) to the Lyman-γ line broadened by H-H$^+$ collisions, which takes into account these new results.

2. Lyman-γ profile calculations

A unified theory of spectral line broadening yields the complete profile from the line center to the far wing, and includes the effect of the dependence of the transition probability on interatomic distance for all states that contribute to the far ultraviolet above Lyman-γ. Complete details and the derivation of the theory are given by Allard et al. (1999). The line shape computed in this way will include contributions from transitions that are weak or asymptotically forbidden as $R \to \infty$ (Allard et al. 2000, 2004a).

In our theoretical work, the spectrum line $F_\nu(\Delta\nu)$ is computed from the Fourier transform

$$F_\nu(\Delta\nu) = \frac{1}{\pi} Re \int_0^{+\infty} \Phi(s) \mathrm{e}^{-i\Delta\nu s} \mathrm{d}s. \quad (1)$$

The Fourier Transform is taken such that $F_\nu(\Delta\nu)$ is normalized to unity when integrated over all frequencies, and $\Delta\nu$ is measured relative to the unperturbed line.

We obtain for a perturber density n_p

$$\Phi(s) = \mathrm{e}^{-n_\mathrm{p} g(s)}, \quad (2)$$

where decay of the autocorrelation function with time leads to atomic line broadening.

The dipole autocorrelation function Φ(s) is evaluated for a classical collision path with an average over all possible collisions. The perturbation of the frequency of the atomic transition during the collision results in a phase shift, $\eta(s)$, calculated along a classical path $R(t)$ that is assumed to be rectilinear. The phase shift is given by

$$\eta(s) = \frac{i}{\hbar} \int_0^s \mathrm{d}t,\ V_{e'e}[R(t)] \quad (3)$$

where $\Delta V(R)$, the difference potential, is given by

$$\Delta V(R) \equiv V_{e'e}[R(t)] = V_{e'}[R(t)] - V_e[R(t)], \quad (4)$$

and represents the difference between the electronic energies of the quasi-molecular transition. For a transition $\alpha = (i, f)$ from an initial state i to a final state f, we have

$$g_\alpha(s) = \frac{1}{\sum_{e,e'}{}^{(\alpha)} |d_{ee'}|^2} \sum_{e,e'}{}^{(\alpha)} \int_0^{+\infty} 2\pi\rho \mathrm{d}\rho \int_{-\infty}^{+\infty} \mathrm{d}x\, \tilde{d}_{ee'}[R(0)] \times [\mathrm{e}^{\frac{i}{\hbar}\int_0^s \mathrm{d}t\, V_{e'e}[R(t)]}\, \tilde{d}^*_{ee'}[R(s)] - \tilde{d}_{ee'}[R(0)]]. \quad (5)$$

The e and e' label the energy surfaces on which the interacting atoms approach the initial and final atomic states of the transition as $R \to \infty$ (R denotes the internuclear distance between the radiator and the perturber). The asymptotic initial and final state energies are E_i^∞ and E_f^∞, such that $E_e(R) \to E_\mathrm{i}^\infty$ as $R \to \infty$.

An H_2^+ correlation diagram was constructed for Lyman-γ to which 14 transitions contribute. Table 1 of Allard et al. (2004b) indicates the states of the united atom correlated to the $n = 1$ and $n = 4$ levels of the separated atoms. The transitions are summarized in Table 2 of Allard et al. (2004b).

We define $\tilde{d}_{ee'}(R(t))$ as a *modulated* dipole (Allard et al. 1999)

$$D(R) \equiv \tilde{d}_{ee'}[R(t)] = d_{ee'}[R(t)] \mathrm{e}^{-\frac{\beta}{2} V_e[R(t)]}, \quad (6)$$

where β is the inverse temperature $(1/kT)$. Here V_e is the ground state potential when we consider absorption profiles, or an excited state for the calculation of a profile in emission.

Our approach requires prior knowledge of accurate theoretical molecular potentials to describe the interaction between radiator and perturber, and also knowledge of the variation in the radiative dipole moment with atom-atom separation for each molecular state.

2.1. Diatomic potentials

The adiabatic interaction of the neutral hydrogen atom and a proton is described by potential energies $V_e(R)$ for each electronic state of the H_2^+ molecule. The H_2^+ molecular potentials were available for the H ($n \leq 3$) states (Madsen & Peek 1971). We had to compute all those related to $n = 4$, the potentials are described in Allard et al. (2004b).

While the position of the line satellites critically depends on the interaction potential, their amplitude depends on both the interaction potential and the radiative dipole moments. In Allard et al. (2004b), we were limited by a lack of knowledge about the dependence of the radiative transition dipole moment on R for each molecular state, the dipole moments $D(R)$ being assumed to remain constant throughout the collision.

2.2. Electric dipole moments

The transition dipole moment matrix element is determined by the following integral:

$$\bar{d}_{ee'}(R) = \int \Psi^*_e(\boldsymbol{r}; R) \boldsymbol{r} \Psi_{e'}(\boldsymbol{r}; R) \mathrm{d}\boldsymbol{r}, \quad (7)$$

where Ψ_e and $\Psi_{e'}$ represent the initial and final state electronic wave functions of H_2^+, respectively, and $\boldsymbol{r}$ is the electron position vector. We precede the internuclear distance R with a ";" to emphasize its role as a parameter in this system.

The most suitable coordinate system for H_2^+ calculations is the prolate spheroidal coordinate system (ζ, η, ϕ). These coordinates are related to x, y, z components of $\boldsymbol{r}$ by the expressions

$$x = \frac{R}{2} \sqrt{(1-\zeta^2)(1-\eta^2)} \cos\phi, \quad (8)$$

$$y = \frac{R}{2} \sqrt{(1-\zeta^2)(1-\eta^2)} \sin\phi, \quad (9)$$

$$z = \frac{R}{2} \zeta\eta. \quad (10)$$

Because of the separability of the Schrödinger equation, the H_2^+ wave functions can be obtained in the form of the simple product

$$\Psi(\boldsymbol{r}; R) = X_{ml}(\zeta; R) Y_{ml}(\eta; R) \frac{\mathrm{e}^{im\phi}}{\sqrt{2\pi}}, \quad (11)$$

where m is the magnetic quantum number, and l is the orbital angular quantum number of the electron in the He^+ ion, that is in the limiting case as $R \to 0$. The wave functions X_{ml} and Y_{ml} as well as the quasi-molecular energy terms are found numerically. For this purpose, expansions over associated Legendre functions and so-called Yaffe-basis are used (Bates & Reid 1968). At large values of R, where the numerical accuracy of this wave function representation decreases, the asymptotic expressions of Kereselidze et al. (2003) are employed.

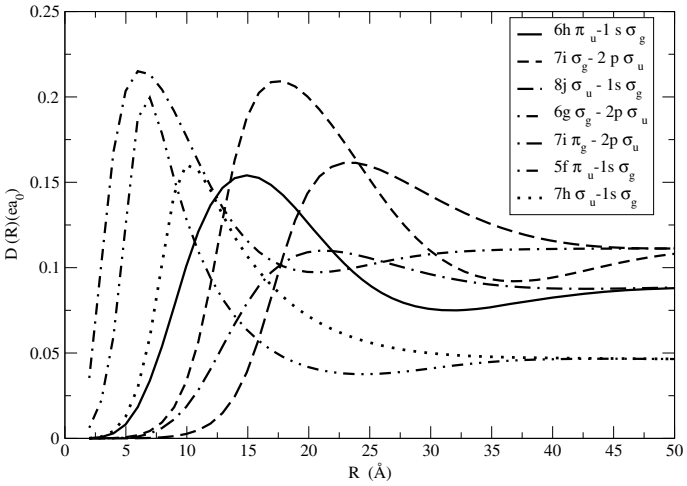

Fig. 1. Electronic transition dipole moments for the satellites of Lyman-γ due to H perturbed by collisions with protons. $D(R)$ is given here in atomic units.

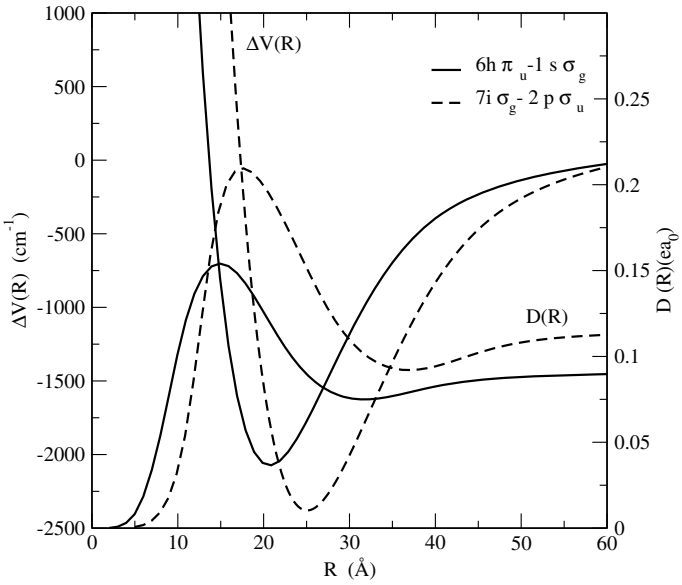

Fig. 2. Difference potential energy ΔV in cm^{-1} for the 992−996 Å satellites and modulated dipoles at $T = 25\,000$ K.

3. Study of the quasi-molecular satellite features

The Lyman-γ profile and its satellites are calculated for the physical conditions encountered in the atmospheres of hot white dwarfs that exhibit the 995 Å structure in their spectra.

The total profile of Lyman-γ depends on the 14 individual transitions, each contribution being given by the Fourier Transform of the autocorrelation function of each component. Those spatial regions for which small changes in the separation of atoms, R, produce little change in the radiated frequency contribute to the appearance of quasi-molecular satellites. Several transitions are of particular interest, and for each one the difference potential exhibits one minimum that, in principle, leads to a corresponding satellite feature in the wing of Lyman-γ.

In Fig. 1, we plot $D(R)$ for these transitions, which all have a dipole moment that increases with decreasing R and goes through a maximum before decreasing to zero when $R \to 0$.

Table 3 of Allard et al. (2004b) lists the wavelengths of these line satellites with the upper and lower state identifications and the distance of the atom-ion pair at which the potential extremum occurs. Several of these features can be identified in the total Lyman-γ profile.

Two transitions, $1s\,\sigma_g \to 6h\,\pi_u$ and $2p\,\sigma_u \to 7i\,\sigma_g$, yield satellites in the red portion of Lyman-γ at 992 Å and 996 Å. An examination of Fig. 2 shows that these line satellites are formed around 20−25 Å. The fast increase in $D(R)$ throughout this region is shown to alter the amplitude of the satellites (Fig. 3). In Fig. 4, we compare the two individual component profiles to the total one for the near wing of Lyman-γ. The two satellites blend in the total profile giving a shape similar to the 995 Å feature observed in WD spectra.

On the other hand, there is no significant increase in the dipole moment in the region of the formation of the line satellites caused by the $8j\,\sigma_u \to 1s\,\sigma_g$ and $6g\,\sigma_g \to 2p\,\sigma_u$ transitions (Fig. 5). The corresponding satellites appear as a wide shoulder on the near wing at 980 Å. In Fig. 6, we present the new Lyman-γ line profile using a variable dipole moment that we compare to the profile obtained in the constant dipole approximation using the asymptotic value of the dipole moment. As expected, there is a significant increase only in the region of the 992 and 996 Å satellites.

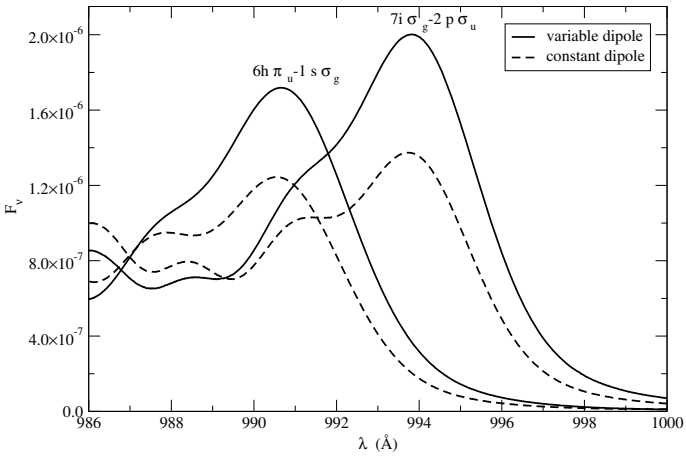

Fig. 3. The 995 Å-region Lyman-γ wing. The individual contribution of the two transitions that give rise to the two main satellites are overplotted in the two theoretical approaches.

4. Synthetic spectra and conclusions

The line profile calculations of Figs. 4 and 6 have been done for a temperature of 25 000 K and a perturber density $n_{H^+} = 1 \times 10^{17}$ cm^{-3}. To highlight the importance of the theoretical improvement in of the line profile calculations, we have displayed in Fig. 7 synthetic spectra for $T_{\rm eff} = 25\,000$ K and $\log g = 8$. The use of opacities calculated with two different approximations concerning the electric dipole transition moment (constant, dependent on interatomic distance) lead to very different synthetic absorption spectra close to 995 Å. As expected, the new Lyman-γ profiles generate deeper absorption in the spectral region of the satellites.

The synthetic spectra have been computed by using the spectral synthesis code SYNSPEC that incorporates the quasi-molecular satellites of Lyman lines. Opacity tables can be obtained from[1].

Atmosphere models have been calculated using the programs TLUSTY (Hubeny 1988; Hubeny & Lanz 1992, 1995). We have

[1] http://mygepi.obspm.fr/~allard/

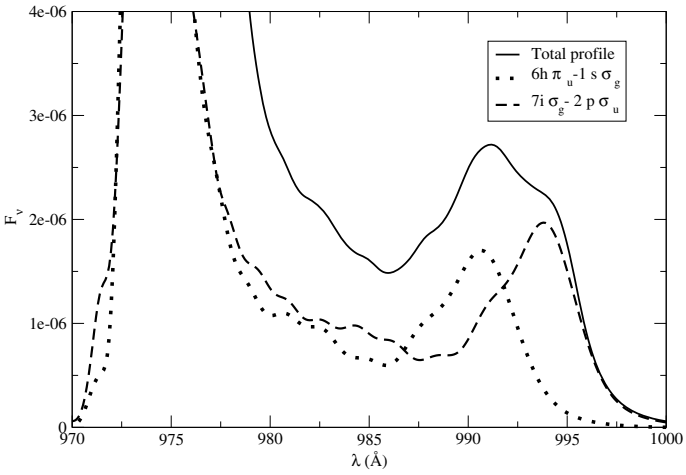

Fig. 4. Total profile of Lyman-γ (T = 25 000 K, n_{H^+} = 1 × 10^{17} cm^{-3}. The individual contribution of the two transitions that give rise to the two main satellites are overplotted.

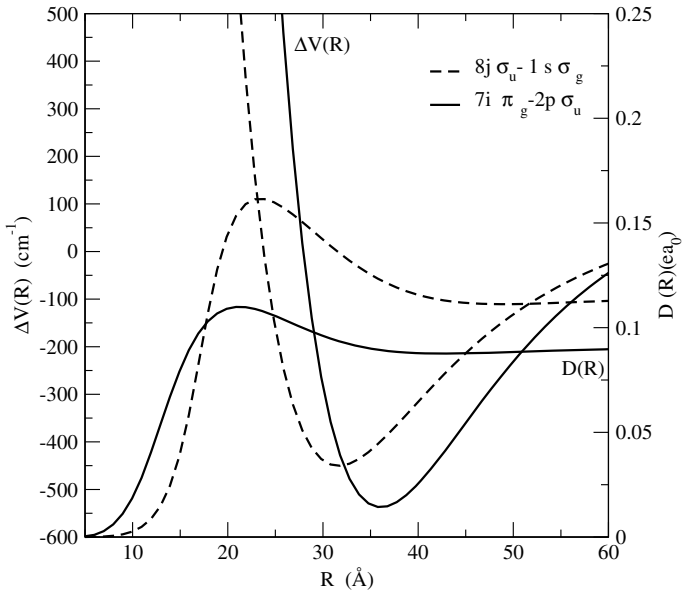

Fig. 5. Difference potential energy $\Delta\omega$ in cm^{-1} for the 978−980 Å satellites and modulated dipoles at T = 25 000 K.

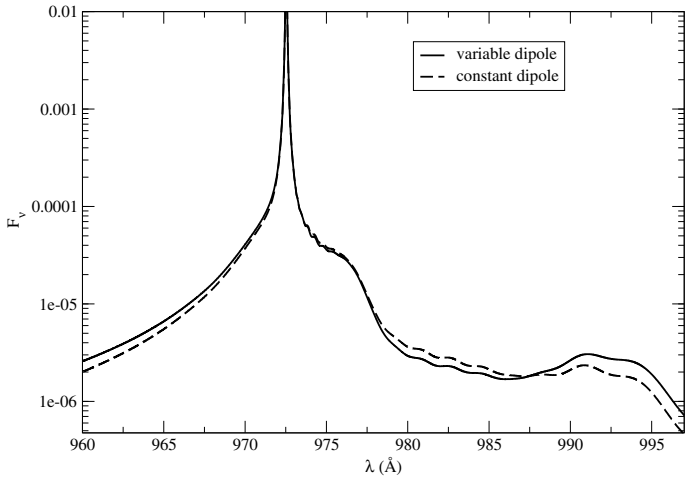

Fig. 6. Lyman-γ profiles with ion density, shown for 1 × 10^{17} cm^{-3} and T = 25 000 K, in the two theoretical approaches. F_ν is the normalized line profile proportional to the absorption coefficient as described by Allard et al. (1999).

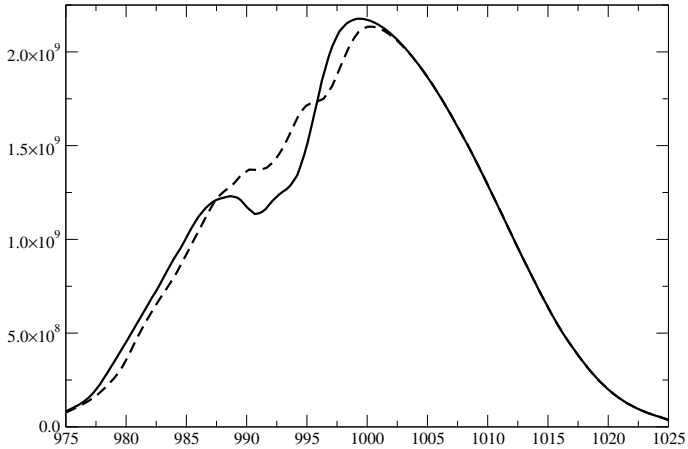

Fig. 7. Synthetic spectra are calculated for log g = 8. and $T_{\rm eff}$ = 25 000 K. Full line: present calculations, dashed line: Allard et al. (2004b) calculations.

considered NLTE model atmospheres with pure hydrogen composition that explicitly include the Lyman-α and Lyman-β quasi-molecular opacities.

Figure 8 compares new theoretical synthetic spectrum with the *FUSE* observations of the white dwarf CD −38°10980. The synthetic spectrum was calculated in NLTE using the parameters determined by Finley et al. (1997), i.e. $T_{\rm eff}$ = 25 276 K and log g = 7.97, and normalized to V = 11.029. The FUSE spectrum shown was produced by merging the data from the LiF1 and SiC1 instrument channels from the observations Q1100101 and C1160202. The raw data were reduced using CalFUSE version 3.2.3, normalized to the LiF1 spectrum of Q110101 at 1050 Å, coaligned with narrow interstellar absorption lines, and combined. The SiC1 data were used only where LiF1 data were unavailable. A major improvement compared to the synthetic spectrum using profiles obtained in the constant dipole approximation calculations (see Fig. 8 of Allard et al. 2004b).

For hotter stars with high gravity, the Lyman-β and Lyman-γ profiles must be evaluated in a unified line shape theory and the density expansion of the autocorrelation function in Eq. (1) that we presently use (Allard et al. 1994) is no longer valid (Allard et al. 2004b). Figures 5 and 6 in Allard et al. (2004b) illustrate the sensitivity of the profiles to the shortcomings of the density expansion approach as the density exceeds 10^{17} cm^{-3}, for the constant-dipole approximation. We anticipate that the magnitude of the discrepancies will be similar for the variable-dipole calculations. This explains the discrepancy between theoretical and observed quasi-molecular satellites in spectra of massive white dwarfs (Dupuis et al. 2003).

The line satellites that appear as shoulders close the unperturbed line center are related to shallow minima at large internuclear distances, whereas the distinct satellites farther from the line center form in the deeper potential wells that occur at a closer atom-ion separation.

The satellites of the higher states are formed by shallow potential extrema at large interatomic separations, and consequently are close to the main line and rapidly become stronger than the main line as the ion density increases. The one-perturber approximation neglects the contribution of the core of the line, and is valid only in the wing, and in the limit of densities that are low enough that multiple perturber effects there may be

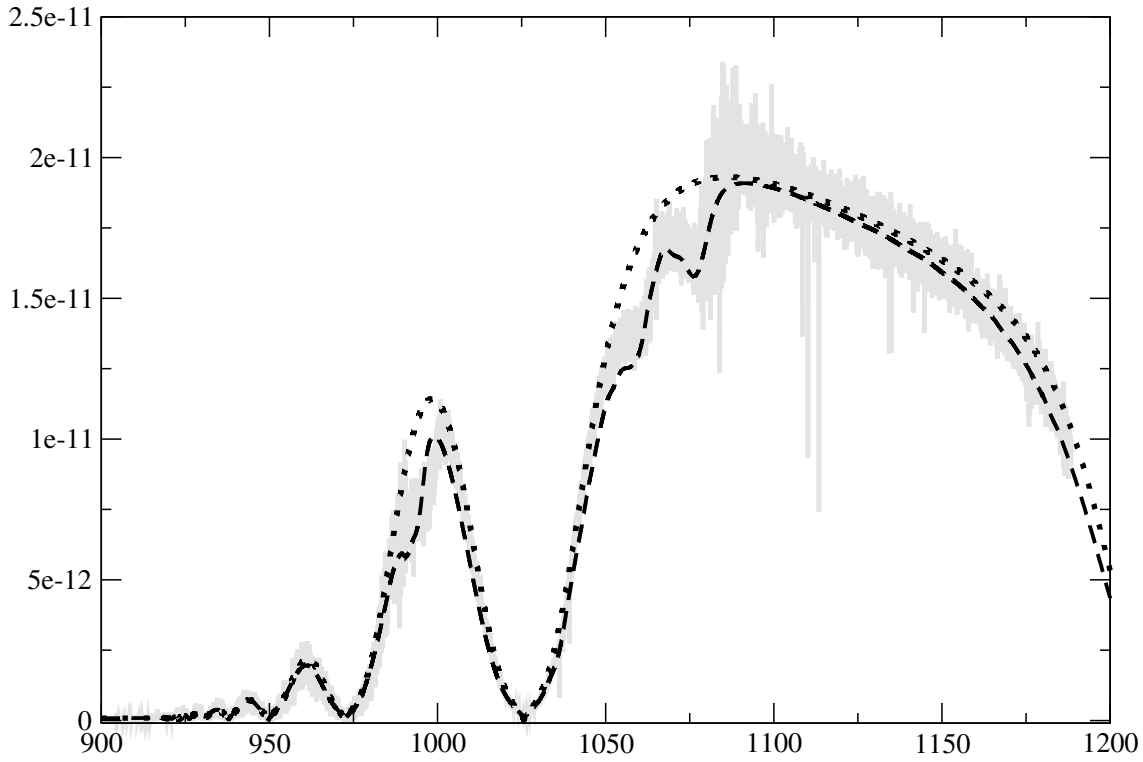

Fig. 8. Comparison of the *FUSE* spectrum of the white dwarf CD −38° 10980 to theoretical models. Synthetic spectra are calculated for $\log g = 7.97$ and $T_{\rm eff} = 25\,276$ K. Dashed line: present calculations, dotted line: with VCS theory.

neglected. In practice, it is not useful in the Lyman series when the the ion density is higher than 10^{17} cm^{-3}. The Lyman-γ opacity table from[2] becomes increasingly unreliable as the ion density exceeds 10^{17} cm^{-3} (see Allard et al. 2004b).

Acknowledgements. N.F.A. is grateful to S. Bourdreux for his help in the study of Lyman-γ profiles.

References

Allard, N. F., & Koester, D. 1992, A&A, 258, 464
Allard, N. F., Koester, D., Feautrier, N., & Spielfiedel, A. 1994, A&AS, 200, 58
Allard, N. F., Drira, I., Gerbaldi, M., Kielkopf, J. F., & Spielfiedel, A. 1998a, A&A, 335, 1124
Allard, N. F., Kielkopf, J. F., & Feautrier, N. 1998b, A&A, 330, 782
Allard, N. F., Kurucz, R. L., Gerbaldi, M., & Faraggiana, R. 1998c, in UV Astrophysics Beyond the IUE Final Archive, Sevilla, November 1997, ESA-SP-413 (Noordwik, The Netherlands: ESA, ESTEC)
Allard, N. F., Royer, A., Kielkopf, J. F., & Feautrier, N. 1999, Phys. Rev. A, 60, 1021
Allard, N. F., Kielkopf, J., Drira, I., & Schmelcher, P. 2000, Eur. Phys. J. D, 12, 263
Allard, N. F., Hébrard, G., Dupuis, J., et al. 2004a, ApJ, 601, L183
Allard, N. F., Kielkopf, J. F., Hébrard, G., & Peek, J. 2004b, Eur. Phys. J. D, 29, 7
Bates, D., & Reid, R. 1968, Adv. At. Mol. Phys., 4, 13
Bergeron, P., Wesemael, F., Lamontagne, R., et al. 1995, ApJ, 449, 258
Dupuis, J., Chayer, P., Vennes, S., Allard, N. F., & Hébrard, G. 2003, ApJ, 598, 486
Finley, D., Koester, D., & Basri, G. 1997, ApJ, 488, 375
Greenstein, J. L. 1980, ApJ, 241, L89
Holberg, J. B., Kruk, J. W., Koester, D., et al. 2003, in White Dwarfs, ed. D. de Martino, R. Silvotti, J.-E. Solheim, & R. Kalytis, NATO ASIB Proc., 105, 113
Holm, A. V., Panek, R. J., Schiffer, F. H., et al. 1985, ApJ, 289, 774
Hubeny, I. 1988, Comp. Phys. Comm., 52, 103
Hubeny, I., & Lanz, T. 1992, A&A, 262, 501
Hubeny, I., & Lanz, T. 1995, ApJ, 439, 875
Kereselidze, T. M., Noselidze, I. L., & Chibisov, M. I. 2003, J. Phys. B: At. Mol. Opt. Phys., 36, 853
Kielkopf, J. F., & Allard, N. F. 1995, ApJ, 450, L75
Koester, D., & Allard, N. F. 1993, in White Dwarfs: Advances in Observation and Theory, ed. M. Barstow, NATO ASIC Proc., 403, 237
Koester, D., Weideman, E.-M., Zeidler, K., & Vauclair, G. 1985, A&A, 142, L5
Koester, D., Finley, D. S., Allard, N. F., Kruk, J. W., & Kimble, R. A. 1996, ApJ, 463, L93
Koester, D., Sperhake, U., Allard, N. F., Finley, D. S., & Jordan, S. 1998, A&A, 336, 276
Madsen, M. M. & Peek, J. M. 1971, At. Data, 2, 171
Nelan, E. P., & Wegner, G. 1985, ApJ, 289, L31
Wolff, B., Kruk, J. W., Koester, D., et al. 2001, A&A, 373, 674

[2] http://mygepi.obspm.fr/allard/